# ARTICLES

## Ultrafast Nonequilibrium Charge Recombination Dynamics of Excited Donor−Acceptor Complexes

**Olivier Nicolet and Eric Vauthey***

*Department of Physical Chemistry, University of Geneva, 30 quai Ernest Ansermet, CH-1211 Geneva, Switzerland*

*Received: January 22, 2002; In Final Form: March 3, 2002*

The dynamics of charge recombination (CR) of excited donor−acceptor complexes composed of methoxy-substituted benzenes and pyromellitic dianhydride were investigated in four different solvents using both the multiplex transient grating and the transient absorption techniques. At constant driving force, the CR dynamics are substantially faster than those with methyl-substituted benzenes as donors. In acetonitrile (ACN), the CR time constant decreases from 3.5 ps with anisole down to 240 fs with tetramethoxybenzene. In valeronitrile, the CR is always slower than in ACN but is, in most cases, faster than diffusional solvation. The free energy, the solvent, and the temperature dependence of the CR dynamics can be qualitatively well reproduced using the hybrid model of Barbara and co-workers after incorporation of the contribution of inertial motion to solvation. The ability of this model to account for the absence of normal region at small driving force is also examined.

### Introduction

Although electron transfer (ET) is certainly the most investigated chemical reaction,[1−3] there are still several unanswered questions. One of them concerns the free energy dependence of the charge recombination (CR) process in excited donor−acceptor complexes (DACs). These species, formed upon charge-transfer excitation, are equivalent to contact ion pairs (CIPs).[4−6] Several investigations have shown that the free energy dependence of CR in excited DACs, or CIPs, deviates substantially from the predictions of the semiclassical treatment of the nonadiabatic ET theory.[7−12] Indeed, the logarithm of the CR rate constant, $k_{CR}$, does not exhibit a quadratic but rather a linear free energy dependence. The DACs investigated by Mataga and co-workers were essentially composed of methylbenzene (MeB) derivatives or of larger polyaromatic hydrocarbons as donors.[7−9] In those cases, the slope of the free energy dependence was around −1.35 decade/eV, independently on the acceptor (tetracyanoanthracene, pyromellitic dianhydride (PMDA), tetracyanoethylene (TCNE)). More recently, Hubig et al. have reported slopes varying from −1.5 with MeBs as electron donors to about 0 decade/eV with olefines.[11]

Several hypotheses have been proposed to account for this discrepancy. Gould et al. explained the linear free energy dependence observed with DACs composed of MeBs/tetracyanobenzene in $CHCl_3$ by a decrease of the solvent reorganization energy, $\lambda_s$, with increasing number of methyl substituents on the donor, i.e., with decreasing driving force.[12] This hypothesis was based on fluorescence band shape analysis. However, this explanation was weakened by Mataga and co-workers, who observed the same linear free energy dependence in polar and non polar solvents as well as on porous glass.[13,14] According to these authors, CR in the excited DACs is rather dominated by intermolecular and intracomplex modes, and thus, the solvent plays a minor role. The results of Hubig et al. are also in disagreement with the hypothesis of Gould et al., as a change of $\lambda_s$ of more than 1 eV would have to be invoked.[11] These authors explain the discrepancy between their data and Marcus theory by the fact that CR in excited DACs is essentially an inner-sphere process and can therefore not be described in terms of the nonadiabatic ET theory.

Another striking feature of the free energy dependence of the CR dynamics of excited DACs is the absence of normal region, i.e., the region at low exergonicity where the rate constant increases with increasing driving force. Indeed, Mataga and co-workers have shown that the linear dependence exists down to a driving force as small as −0.5 eV,[7] whereas nonadiabatic ET theory predicts a strong decrease of $k_{CR}$ with decreasing driving force below ∼−1.5 eV. The latter behavior has been reported for geminate ion pairs (GIPs) formed by diffusional ET quenching.[15,16]

Tachiya and Murata have explained this behavior by a mechanism where CR occurs in parallel to solvent relaxation after formation of the CIP far from equilibrium.[17] However, to reproduce the linear dependence down to very low exergonicity, an unrealistically large electronic coupling constant had to be invoked. Moreover, this model predicts a nonexponential decay of the excited-state population, in disagreement with the experimental data of Mataga and co-workers.[7−9]

More recently, Frantsuzov and Tachiya have proposed a model where CR is described as a transition between two adiabatic surfaces.[18] Laser excitation produces a nonequilibrium

* To whom correspondence should be addressed. E-mail:eric.vauthey@chiphy.unige.ch.

10.1021/jp025542c CCC: $22.00 
Published on Web 05/17/2002

**TABLE 1: Static Dielectric Constant, $\epsilon_s$, Viscosity, $\eta$, and Diffusional Solvation Time, $\tau_{ds}$, of the Solvents**

| | ACN | ACE | VaCN | EtAC |
|---|---|---|---|---|
| $\epsilon_s$[a] | 37.5 | 20.7 | 19.7 | 6.0 |
| $\eta$ (cP)[a] | 0.345 | 0.304 | 0.693 | 0.426 |
| $\tau_{ds}$ (ps) | 0.50[b] | 0.83[b] | 4.7[c] | 2.63[b] |

[a] Ref 26. [b] Ref 23. [c] Ref 29.

initial population on the upper surface and, in the normal region (weak free energy), the transition from the upper to the lower surface can proceed without an activation barrier. In this model, the electronic coupling constant is smaller and an exponential population decay is predicted.

Nonequilibrium ET dynamics has already been reported by several groups.[19−22] Barbara and co-workers have developed a hybrid model that allowed the solvent and temperature dependence of ET in betaines and in mixed valence compounds to be qualitatively accounted for.[21,23−25] However, the prediction of this hybrid model concerning the free energy dependence of the ET dynamics was not explored.

We report here on our investigation of the CR dynamics of excited DACs composed of PMDA as acceptor and methoxy-substituted benzene (MoB) derivatives as donors in acetonitrile (ACN), acetone (ACE), valeronitrile (VaCN), and ethyl acetate (EtAc). ACE and VaCN have a similar polarity but a different viscosity, while ACE and EtAc have a similar viscosity but a different polarity (see Table 1).[26] For the sake of comparison, the system *p*-xylene/PMDA was also studied.

MoBs have been chosen for two reasons: (1) The CR dynamics of GIPs formed by ET quenching with MoBs is much faster than that measured with MeBs at constant driving force.[27] Therefore, the CR dynamics in excited DACs composed of MoBs/PMDA can also be expected to be substantially faster than the MeBs/PMDA DACs investigated by Mataga and co-workers.[13] (2) It was recently found that the CR dynamics of GIPs formed by ET quenching at high donor concentration can be analyzed within the framework of the nonadiabatic ET theory if the GIPs are sorted according to the electron donor.[28] The CR rate constants measured with all MoBs could be well described with a single set of parameters. It was also found that at high donor concentrations, the resulting GIPs were rather contact ion pairs (CIPs) and not solvent separated ion pairs.

The aims of this study are as follows: (1) to investigate whether the free energy dependence of CR in the excited DACs composed of MoBs/PMDA is bell-shaped as that observed in above-mentioned CIPs, or linear (in a logarithmic scale) as observed in other DACs; (2) to investigate whether the solvent, which plays a minor role in the moderately fast CR dynamics of MeBs/PMDA DACs, has a larger influence when the CR is faster; and (3) to get more insight into the role of nonequilibrium effects on the free energy dependence of ET.

## Experimental Section

**Apparatus.** The CR dynamics of excited DACs has been investigated using both multiplex transient grating (TG) and transient absorption (TA). Excitation was performed using the frequency doubled output of a standard 1 kHz amplified Ti: Sapphire system (Spectra-Physics). The duration of the pulses at 400 nm was around 100 fs. The multiplex TG setup has been described in details elsewhere.[28] All TG spectra were corrected for the chirp of the probe pulses.[28]

For TA, the pump pulses at 400 nm were sent along an optical delay line before being focused with a 100 mm achromatic lens onto the sample, located 20 mm in front of the focal point. A fraction of the unconverted light at 800 nm, was focused with a 100 mm lens in a 5 mm thick sapphire window for supercontinuum generation. The resulting output was recollimated and split in two parts. The first one, used as a reference, was passed through an interference filter and focused on a photodiode. The second part, which was used for probing, was focused on the sample with the same lens as that used for the pump pulses. After the sample, it was filtered with either an interference filter or a 100 mm monochromator and focused on a second photodiode. The output of both signal and reference photodiodes was amplified and directed to a computer board for digitization (Axiom 5210 A/D board).[30] The pump energy on the sample was around 20 $\mu$J with a spot size of 0.7 mm diameter. The width (fwhm) of the response function of this setup was around 200 fs.

For both experiments, the probe light was polarized at magic angle relative to the polarization of the pump pulses.

**Data Analysis.** The time profiles of the TA and TG intensity were analyzed by iterative reconvolution using the following equation

$$I(t) = \int_{-\infty}^{+\infty} I_{pr}(t - t'')[\int_{-\infty}^{t} R(t' - t) I_{pu}(t') dt']^n dt'' \quad (1)$$

where $n = 1$ for TA and $n = 2$ for TG, $I_{pu}$ and $I_{pr}$ are the intensities of the pump and probe pulses, respectively, and $R$ is the response of the sample. The integral in the square brackets is the convolution of the sample response with the pump pulse, whereas the first integral is the convolution with the probe pulse.

**Samples.** Pyromellitic dianhydride (PMDA) was recristallized and sublimed and 1,4-dimethoxybenzene (DMB) was recristallized. Anisole (ANI), veratrole (VER), 1,2,4-trimethoxybenzene (TrMB), and *p*-xylene (PXY) were distilled, whereas 1,2,4,5-tetramethoxybenzene (TeMB) was synthesized as described in the litterature.[31] Perdeuterated *p*-xylene ($PXY_d$, Cambridge Isotopes) was used as received. Acetonitrile (ACN), acetone (ACE), and ethyl acetate (EtAc) were of spectroscopic grade and were used without further purification, whereas valeronitrile (VaCN) was purified as described in the litterature.[32] Unless specified, all compounds were from Fluka.

The concentration of PMDA was around 0.15 M and that of the donors was adjusted to obtain an absorbance at 400 nm of about 0.2 over 1 mm, the sample thickness. This corresponds to concentrations of 0.3 M with the weaker donors (PXY and ANI) and of less than 0.2 M with the others. The formation of 1:1 complexes was confirmed by Job plots.[33,34]

During the experiment, the samples were continuously stirred by $N_2$ bubbling. No significant sample degradation was observed after the measurements.

## Results

**Steady-State Measurements.** Solutions containing both PMDA and an electron donor exhibit a new broad absorption band, whose maximum is strongly correlated with the oxidation potential of the donor as shown in Table 2. This new absorption feature can be ascribed to a charge transfer (CT) transition of the DAC. Even with the strongest donors, the CT band is not well separated from the absorption bands of the constituents. With weak donors, like PXY and ANI, only the low energy side of the CT band can be observed and the maximum cannot be clearly distinguished. On the other hand, with the strongest donors, like TeMB and TMB, the onset of a second band at higher energy can be observed. Attempts to isolate the absorption band of the DAC by subtracting the PMDA and donor spectra were not successful. This is most probably due to the

**TABLE 2: Oxidation Potential of the Electron Donors, $E_{ox}$(D), and Maximum of the CT Absorption Band of the D/PMDA Complexes, $\lambda_{CT}$, in ACN**

| donor | $E_{ox}$ (V vs SCE) | $\lambda_{CT}$ (nm) |
|---|---|---|
| PXY | 2.06[a] | < 350 |
| ANI | 1.76[a] | ~ 365 |
| VER | 1.45[b] | ~ 395 |
| DMB | 1.34[b] | 415 |
| TrMB | 1.12[b] | 450 |
| TeMB | 0.81[b] | 490 |

[a] Ref 35. [b] Ref 36.

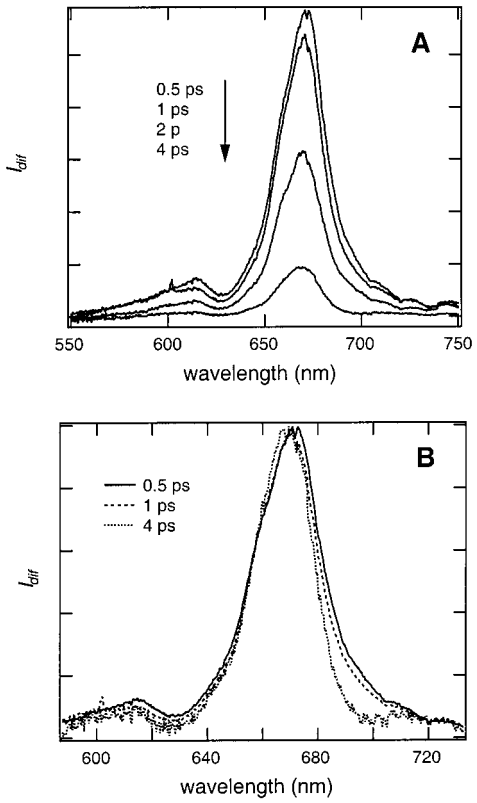


**Figure 1.** (A) TG spectra measured with ANI/PMDA in ACN at different time delays after excitation. (B) Same as in A but intensity normalized spectra.

spectral shift of the PMDA absorption band in the presence of the aromatic donors, whose refractive index differs substantially from those of the solvents used.

The DAC spectra do not exhibit a very significant change by going from the polar ACN to the weakly polar EtAc. This is in agreement with a small permanent dipole moment of the D/PMDA complexes in the ground state.

**Transient Grating Spectra.** Figure 1A shows the chirp corrected TG spectra measured after excitation at 400 nm in the CT band of the ANI/PMDA complex. The nature of a TG spectrum has been discussed in details elsewhere.[37] In brief, the TG intensity is proportional to the square of the photoinduced absorbance and refractive changes. Consequently, the TG spectrum is the sum of the squares of the TA and of the transient dispersion spectra. Practically, the TG spectrum is very similar to the corresponding TA spectrum, the major difference being that the former is always positive. The major advantage of TG over TA is its superior sensitivity, due to the zero-background nature of this technique. At short time delay, when the pump and probe pulses temporally overlap, the TG signal contains additionally a nonresonant contribution from the solvent, essentially related to the electronic optical Kerr effect.[38] This response is instantaneous compared to the pulse duration and its contribution appears as a broad and structureless spectrum at time zero. This nonresonant background spectrum can interfere with the resonant contribution and distort the TG spectra. Consequently, the TG spectra measured at time delays shorter than about 500 fs have not been considered.

At longer time delays, the TG spectrum consists of an intense band centered around 670 nm with a smaller band at about 612 nm. This spectrum compares very well with the absorption spectrum of $PMDA^{\bullet-}$ measured in liquids and in solids matrices.[13,39,40]

Figure 1B shows the intensity normalized TG spectra measured with the same DAC in ACN. Some spectral dynamics can be clearly observed: as the time delay increases, the band becomes narrower, the band maximum shifts to shorter wavelengths and the relative intensity of the 612 nm band decreases. However, the very short lifetime of this transient (vide infra) makes the analysis of the spectral dynamics difficult. For this reason, the spectral dynamics has been investigated with PXY/PMDA, which has a longer excited-state lifetime.[13] Figure 2A shows the contour plot of the normalized TG intensity measured with PXY/PMDA in EtAc upon 400 nm excitation. The intensity normalization has been done relative to the maximum of the 670 nm band. Both the band narrowing and the peak shift can be very clearly discerned. Figure 2B, shows the time dependence of the full width at half-maximum (fwhm) of the square root of the 670 nm TG band. This profile can be well reproduced by a biexponential function with 1.2 and 50 ps time constants. Figure 2C indicates that the maximum of the TG band exhibits a quite similar time dependence. As the total shift is rather small, only a very approximate time constant can be extracted. As illustrated in Figure 2D, the square root of the relative TG intensity of the 612 nm band is also time dependent. This change is not very large, but seems to occur in the same time scale as the band narrowing and the peak shift. The time constants pertaining to these spectral changes in the four solvents are listed in Table 3.

These TG measurements have also been performed using VER, DMB, TMB, and TeMB as electron donors in ACN, ACE, VaCN, and EtAc. The same TG bands around 670 and 612 nm were found with each system and in all solvents investigated. Spectral changes similar to those mentioned above could also be observed. However, their amplitudes were smaller due to the shorter lifetime of the transient. Nevertheless, their time scale did not appear to depend significantly on the electron donor.

**Excited DAC Dynamics.** Figure 3 shows the time profiles of the square root of the diffracted intensity measured with PXY/PMDA, ANI/PMDA, and DMB/PMDA in ACN. For XY/PMDA and ANI/PMDA, the time profile was measured at 657 nm. The TG intensity at this wavelength is not influenced by the spectral dynamics as shown in Figure 1B. For shorter lived transient, there is almost no spectral dynamics. As mentioned above, the TG intensity at short time delay is somehow "contaminated" by the nonresonant contribution of the solvent. This contribution can be measured separately with the solvent alone. As explained in more detail in previous publications,[28,41] the removal of this contribution by subtraction from the total TG intensity is only valid at the maximum of the TG bands. Consequently, the dynamics of the TG intensity with this very short-lived excited DACs has been measured at the band maximum, and the nonresonant contribution of the solvent has been removed.

The reliability of this procedure was confirmed by TA absorption measurements at 670 nm (see Figure 3D). The lower signal-to-noise ratio of the TA time profile is compensated by

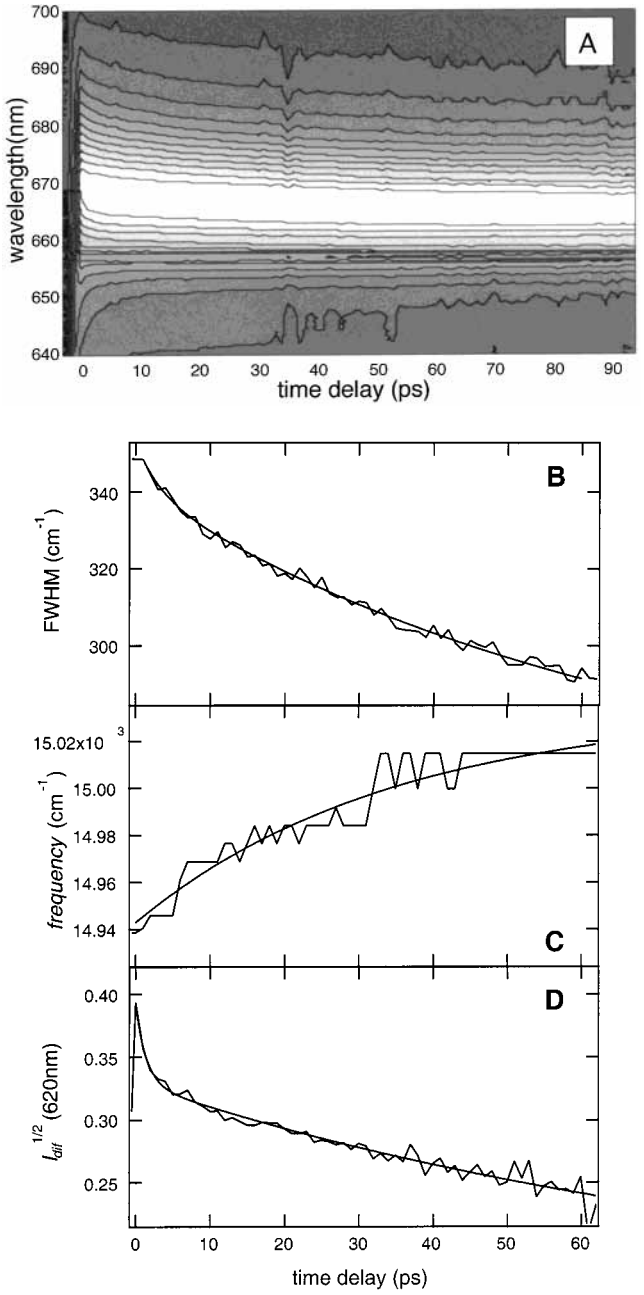


**Figure 2.** (**A)** Contour plot of the TG intensity normalized at the band maximum measured with PXY/PMDA in EtAc. Time dependence of **(B)** the full width at half-maximum of the square root of the 670 nm band, **(C)** the frequency shift of the 670 nm TG band maximum and **(D)** of the square root of the relative intensity of the 620 nm band, together with best biexponential (B and D) and single exponential (C) fits.

**TABLE 3: Time Constants Related to the Spectral Dynamics Measured with PXY/PMDA: Full Width at Half Maximum, $\tau$(fwhm), Shift of the 670 nm TG Band Maximum, $\tau$(shift) and Relative Intensity of the Square Root of the 612 nm Band, $\tau$(612)**

| solvent | $\tau$(fwhm) (ps) | $\tau$(shift) (ps) | $\tau$(612) (ps) |
|---|---|---|---|
| ACN | 1.1 (21%) + 11 (79%) | 11 | 1 (15%) +14 (85%) |
| ACE | 1 (28%) + 7.2 (72%) | 9 | 1(23%) + 8 (77%) |
| VaCN | 2 ps (24%)+ 34 ps (76%) | 38 | 2 (22%)+ 35 (78%) |
| EtAc | 3 ps (17%)+ 58 ps (83%) | 44 | 1.2 (19%) + 50 (81%) |

the absence of any interference effect at short time delay. The analysis of both TG and TA time profiles resulted in very similar kinetic parameters.

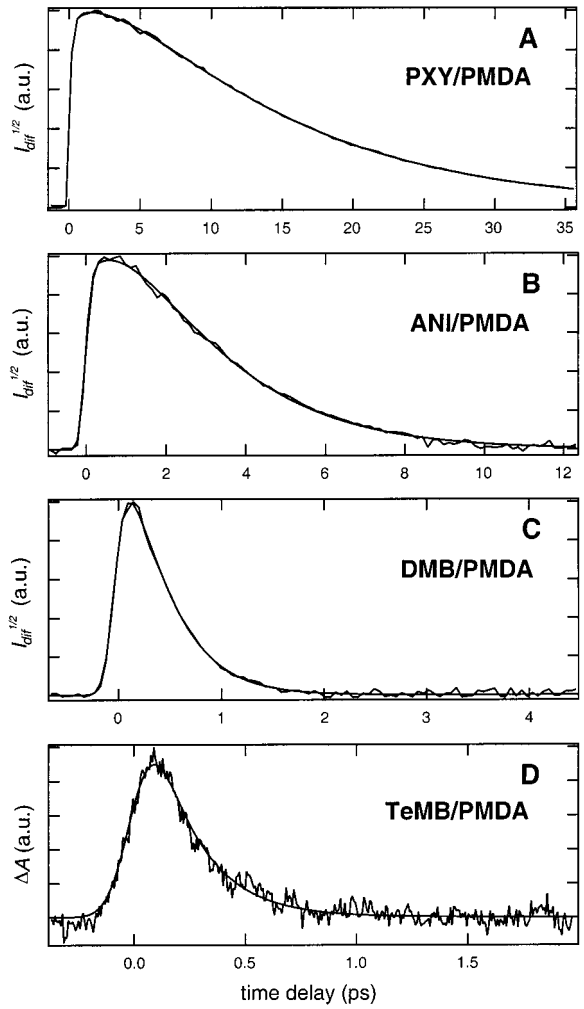


**Figure 3.** (A)−(C) Time profiles of the square root of the TG intensity measured with several D/PMDA DACs in ACN, and (D) time profile of the transient absorption at 670 nm measured with TeMB/PMDA in ACN.

**TABLE 4: Rise Time, $\tau_R$, and Decay Time, $\tau_D$, in ps, of the Excited D/PMDA DAC Population in Various Solvents**

| donor/ solvent | ACN | ACE | VaCN | EtAc |
|---|---|---|---|---|
| PXY | $\tau_R$ = 1.2 | $\tau_R$ = 1.5 | $\tau_{R,1}$ = 2.1 (5%) | $\tau_{R,1}$ = 2.0 (15%) |
| | | | $\tau_{R,2}$ = 11.6 (55%) | $\tau_{R,2}$ = 13.8 (45%) |
| | $\tau_D$ = 12.0 | $\tau_D$ = 12.6 | $\tau_D$ = 24.0 | $\tau_D$ = 63.1 |
| ANI | $\tau_R$ = 0.58 | $\tau_R$ = 1.3 | $\tau_R$ = 2.9 | $\tau_R$ = 4.1 |
| | $\tau_D$ = 3.55 | $\tau_D$ = 4.30 | $\tau_D$ = 8.32 | $\tau_D$ = 13.8 |
| VER | $\tau_R$ = 0.16 | $\tau_R$ = 0.66 | $\tau_R$ = 0.84 | $\tau_R$ = 0.90 |
| | $\tau_D$ = 0.85 | $\tau_D$ = 1.70 | $\tau_D$ = 2.40 | $\tau_D$ = 3.40 |
| | | | $\tau_R$ = 0.5 | |
| DMB | $\tau_D$ = 0.50 | $\tau_D$ = 0.97 | $\tau_D$ = 1.66 | $\tau_D$ = 2.0 |
| TrMB | $\tau_D$ = 0.34 | $\tau_D$ = 0.57 | $\tau_D$ = 1.0 | $\tau_D$ = 1.05 |
| TeMB | $\tau_D$ = 0.24 | $\tau_D$ = 0.32 | $\tau_D$ = 0.42 | |

Figure 3 shows that, with the weaker donors, the TG signal does not reach its maximum intensity instantaneously. Most of these time profiles could be reproduced using a biexponential function, with a small rising component and a component decaying to zero. The fitting parameters, listed in Table 4, indicate that the decay time decreases markedly with the oxidation potential of the donor. The rising component shows a similar trend. As a consequence, the time profiles measured with the strongest donors can be reproduced using a single-exponential function.

The small amplitude of the rising component does not allow a very precise analysis. The actual rising dynamics might more

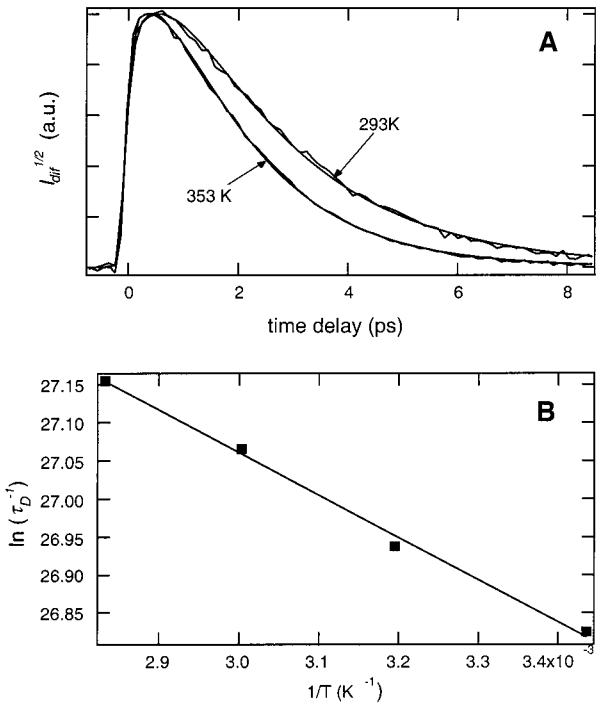


**Figure 4.** (A) Time profiles of the square root of the TG intensity at 657 nm measured with VER/PMDA in VaCN at two temperatures. (B) Arrhenius plot of the inverse lifetime of the excited VER/PMDA in VaCN.

**TABLE 5: Activation Energy Determined from the Temperature Dependence of the Excited D/PMDA Population Decay, $E_A^{obs}$, and Calculated According to the Hybrid model, $E_A^{calc}$ (error on $E_A^{obs} \approx \pm$ 10 MeV)**

| donor | solvent | $E_A^{obs}$ (meV) | $E_A^{calc}$ (meV) |
|---|---|---|---|
| ANI | ACN | 32 | 26 |
| PXY | VaCN | 34 | 31 |
| ANI | VaCN | 54 | 40 |
| VER | VaCN | 50 | 38 |
| DMB | VaCN | 45 | 34 |

complex than just monoexponential. This quite clear in the case of PXY/PMDA in EtAc and VaCN, where the rise is the most marked, and is clearly biphasic.

**Temperature Effect.** The effect of temperature on the excited DAC dynamics was investigated with a few DACs in VaCN and ACN. Figure 4A illustrates the influence of temperature on the time profile of the TG intensity measured with VER/PMDA in VaCN and Figure 4B shows that the decay time of the excited DAC follows an Arrhenius type temperature dependence. The resulting activation energies for this DACs and for the other systems investigated are listed in Table 5. The variation of the decay time with temperature is weak and therefore the error on the activation energy is relatively large. An Arrhenius type temperature dependence of the rising component could also be observed with PXY/PMDA in VaCN. The corresponding activation energy amounts to 100 ± 10 meV.

**Deuterium Isotope Effect.** Perdeuteration of PXY has a marked effect on the excited DAC dynamics. The decay time of the excited DAC increases substantially with perdeuteration. In VaCN, it increases from 38 ps with PXY to 72 ps with $PXY_d$. The same relative change was observed in EtAc, the decay time going from 70 ps with PXY to 145 ps with $PXY_d$. On the other hand, the rising component of the TG signal did not exhibit any significant change upon isotope substitution of the donor.

## Discussion

**Spectral Dynamics.** As shown in Table 3, the narrowing, the shift and the change of the relative magnitude of the 612 nm TG band occur in a similar time scale, which is clearly solvent dependent. Therefore, these three different spectral changes must problably have the same origin. Time dependent absorption spectra of $PMDA^{\bullet -}$ in frozen glasses have already been observed by Huddleston and Miller.[42] The absorption band of $PMDA^{\bullet -}$ prepared by $\gamma$-irradiation in a methyltetrahydrofuran glass at 82 K, was reported to exhibit a shift from 680 to 670 nm in time scales ranging from 100 ns to 100 s. This effect was ascribed to the reorientation of the anion in the glassy matrix.

Excitation of a DAC results in the formation of a CIP with the equilibrium intramolecular and solvent coordinates of the ground state. The negligibly small solvent dependence of the D/PMDA CT absorption band implies that there is essentially no CT in the ground state and therefore that the CIPs are initially formed far from their equilibrium configuration. In principle, excitation at the maximum of the CT band populates the excited state with an excess energy corresponding to the total reorganization energy for ET, $\lambda$.[43] Consequently, a substantial relaxation of both intramolecular and solvent modes should occurs directly after excitation.

The relaxation of high frequency intermolecular modes is ultrafast and should not be responsible for the observed spectral dynamics. However, this intramolecular vibrational relaxation leads to a vibrationally hot excited DAC. The temperature of an excited D/PMDA complex after intramolecular vibrational redistribution of 0.4 eV can be estimated to be around 400 K. The cooling of this hot complex by interaction with the solvent occurs typically in about 10 ps, as shown by recent investigations.[44−46] This could somehow account for the spectral dynamics observed in ACN and ACE. In VaCN and EtAc however, the time constants of the spectral dynamics are certainly too large to be explained by vibrational cooling.

The relaxation of solvent modes is essentially biphasic. Indeed, it has been shown that a large fraction of solvation occurs via inertial motion of the solvent molecules.[47−49] This motion is independent of the solvent viscosity and is ultrafast. The remaining solvation involves diffusional motion of the solvent molecules and thus depends on viscosity. The diffusional solvation times, $\tau_{ds}$, of ACN and ACE are smaller than 1 ps,[50] whereas $\tau_{ds}$ values of 2.6 and 4.7 ps have been reported for EtAc and VaCN, respectively (see Table 1).[23,29] Consequently, solvation could somehow account for the fast component of the spectral dynamics but is clearly too fast to explain the slow component.

Spectral narrowing of the transient absorption band after excitation of several DACs in ACN has also been reported by Mataga and co-workers.[10] These authors have ascribed this effect to structural changes of the excited DAC, and more precisely to an increase of the interionic distance from 3.5 Å to about 6 Å. Structural changes involving diffusional motion, rotation and/or translation, are in good agreement with the time scale of the relatively slow spectral dynamics observed here. For example, the reorientation time of PXY, calculated using the Stokes−Einstein−Debye equation and assuming a spherical molecular shape, ranges from 8 ps in ACE to 20 ps in VaCN. The same trend is obtained for translational diffusion. Therefore, the relative magnitude of the time constants for the spectral dynamics in ACE and VaCN could, to a large extent, be accounted for by such structural changes. Changes involving rotational diffusion only cannot explain the slow spectral

dynamics observed in EtAc, whose viscosity is similar to that of ACN and ACE. However, the dynamics of translational diffusion of two oppositely charged species depends strongly on solvent polarity.[51] In polar solvents, the loss of electrostatic stabilization energy upon separating the charges is compensated by a gain in solvation energy. Therefore, such a solvent assisted structural change leading to a slight increase of the interionic distance can be expected to be faster in a polar than in a low polar solvent like EtAc.

Table 4 shows that the lifetime of the excited DACs with MoBs as donors is substantially smaller than the time constant of the slow component of the spectral dynamics. This indicates that the structure of the excited state, and especially the interionic distance, remains almost constant and close to that of the ground-state complex.

**Nature of the Slow Rising Component.** As shown in Figures 3 and 4, the intensity of the 670 nm band does not reach its maximum instantaneously but exhibits a slow rising component. Such a behavior has been observed with other excited DACs[10,52,53] and has been attributed to the relaxation of the excited DACs from the Franck−Condon to the equilibrium configuration. Table 4 shows that this rise time in not only solvent dependent as reported by Jarzeba and co-workers,[52] but varies also substantially with the strength of the electron donor. The activation energy obtained from the temperature dependence of the rise time with PXY/PMDA in VaCN amounts to 100 ± 10 meV and is the same as that related to the viscosity of this solvent.[54] This similarity indicates that the rise must be connected to a diffusional process, like solvation and structural changes as discussed above. For PXY/PMDA in ACN and ACE, the rise time is similar to the time constant related to the faster component of the spectral dynamics and ascribed to solvation. In EtAc and VaCN, the rise was clearly biphasic and the fast component can also be compared with the fast component of the spectral dynamics. However as stated above, both the spectral dynamics and the rise could be more complex and involve a wide distribution of time constants. In this case, only the rising components with a time constant shorter than the excited-state lifetime can be observed. This might explain the observed correlation between the rise time and the strength of the donor.

**Nature of the Decay.** The decay of the TG intensity can be unambiguously ascribed to the decrease of the excited DAC population upon CR to the ground state. Excited DACs have essentially two nonradiative deactivation channels: CR to the ground state and dissociation to free ions.[55] The latter process is diffusional and occurs typically in the sub-ns to ns time scale in ACN[27,56] and in a longer time scale in more viscous and/or less polar solvents.[57] Considering that in ACN the largest decay time is inferior to 5 ps, this process cannot be significantly involved in the dynamics of the MoB/PMDA DACs, as already discussed above. This is confirmed by the fact that the TG intensity decays to zero. If dissociation was really playing a role, it would result to the formation of a long-lived free ion population. In this case, the TG signal would decay to a value different from zero, which would remain constant in the time window of our experiment. Such time profiles have been observed, for example, with geminate ion pairs, whose CR occurs in a similar time scale as dissociation.[27,56] The nature of the decay is further confirmed by the observation of a deuterium isotope effect on the excited-state lifetime. The effect of deuterium substitution is to decrease the Franck−Condon factor between the excited and ground states of the DACs and therefore to slow CR, especially in the inverted region. Deuterium isotope

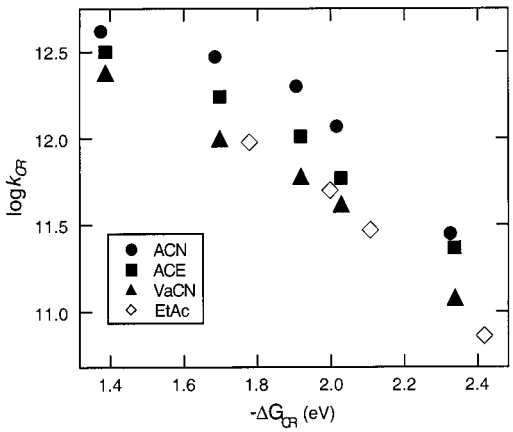


**Figure 5.** Free energy and solvent dependence of the CR rate constant of excited MoB/PMDA complexes.

effects in CR reactions have already been observed with GIPs,[58] exciplexes[59] and excited DACs.[60] An effect with a very similar magnitude as that measured here has been reported with PXY/tetracyanobenzene in a nonpolar solvent.[60]

Fluorescence is not a significant deactivation pathways of excited DACs. The oscillator strength of the CT transition of most DACs is very small, and therefore, the corresponding radiative lifetime is of the order of several hundreds of ns. Apart from PXY/PMDA, for which a very weak emission was observed in EtAc, no fluorescence could detected with the DACs studied here, indicating a fluorescence quantum yield inferior to about $10^{-5}-10^{-6}$, in agreement with the very short excited-state lifetime of these species.

Consequently, the rate constant of CR, $k_{CR}$, was calculated as the inverse of the excited DAC lifetime, $k_{CR} = 1/\tau_D$.

**Free Energy and Solvent Dependence of the CR.** Figure 5 shows the logarithm plot of the rate constant $k_{CR}$ as a function of the free energy, $\Delta G_{CR}$. The latter was calculated using the following empirical eq[61]

$$\Delta G_{CR} = E_{ox}(D) - E_{red}(A) + \frac{0.56\text{eV}}{\epsilon_s} \qquad (2)$$

where $E_{ox}$(D) and $E_{red}$(A) are the oxidation and reduction potentials of the donor and acceptor, respectively, and $\epsilon_s$ is the static dielectric constant of the solvent. This relationship, based on an expression proposed by Weller,[62] was established for the PXY/tetracyanobenzene DAC and can be expected to be also valid for the DACs investigated here. In polar solvents, the last term on the rhs of this equation is almost negligible.

Figure 5 shows that $k_{CR}$ increases continuously with decreasing driving force. In ACN, the logarithmic plot of the $k_{CR}$ is clearly not linear, contrarily to those observed with many DACs.[7−9,11,12] Interestingly, the free energy dependence of log$k_{CR}$ seems to become more linear in ACE and especially in VaCN. In the latter solvent, the slope of the free energy dependence amounts to −1.34 decade/eV and is the same as that reported by Mataga and co-workers for several types of DACs.[7−9] However, the physical meaning of such free energy plots is highly questionable. Indeed, the calculated free energies correspond to states at equilibrium and, from the above discussion, is it quite clear that the excited DACs are formed out of equilibrium and that CR can occur before equilibrium is established. As a consequence, the actual driving force for CR is time dependent and decreases as the excited state population relaxes to eventually reach the equilibrium value, as depicted

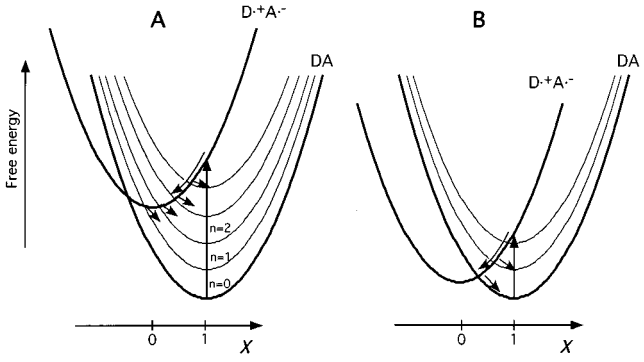


**Figure 6.** Illustration of the hybrid model using cuts in the free energy surfaces of the ground and excited states of a DAC along the solvent coordinate for (A) the inverted and (B) normal regimes.

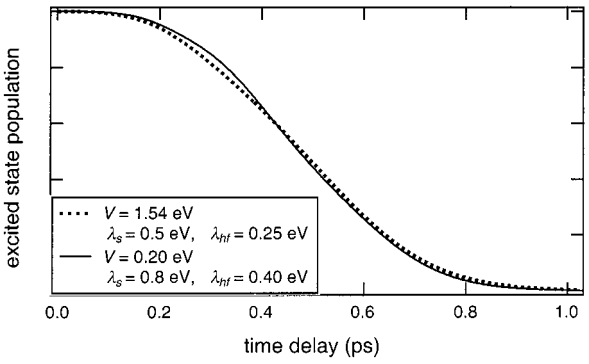


**Figure 7.** Time evolution of the excited DAC population in ACN calculated using eq 3 with two different sets of parameters resulting in $\tau_e$= 500 fs.

in Figure 6A. Therefore, $k_{CR}$ can be expected to be time dependent as well and, in the inverted regime, to increase as relaxation occurs.

Barbara and co-workers have proposed a hybrid model to describe the dynamics of such nonequilibrium charge-transfer processes.[23,25] It combines the classical Sumi-Marcus model,[63] which considers ET processes occurring in parallel to solvation, with the semiclassical model of Jortner and Bixon,[64] which describes the high-frequency intramolecular modes quantum-mechanically.

In the hybrid model, the CR rate constant depends on the solvation coordinate $X$[23]

$$k_{CR}(X) = \frac{2\pi}{\hbar}V^2(4\pi\lambda_{lv}k_BT)^{-1/2}\sum_n \frac{S^n}{n!}\exp(-S) \times \exp\left[-\frac{\Delta G^{\ddagger}_{0\to n}(X)}{k_BT}\right] \quad (3)$$

where $V$ is the electronic coupling matrix element, $\lambda_{lv}$ is the reorganization energy of the low-frequency vibrational modes, which are treated classically, $S$ is the Huang−Rhys factor and corresponds the average number of vibrational quanta excited in the final state. This value can also be expressed as $S = \lambda_{hv}/h\nu$, where $\lambda_{hv}$ is the reorganization energy associated to the high-frequency vibrational modes and $\nu$ is the average frequency of the vibrational modes coupled to ET. The $X$ dependence of $k_{CR}$ is essentially contained in the activation free energy $\Delta G^{\ddagger}_{0\to n}$

$$\Delta G^{\ddagger}_{0\to n}(X) = \frac{[\Delta G_{CR} + nh\nu + (1-2X)\lambda_s]^2}{4\lambda_{lv}} \quad (4)$$

where $\Delta G_{CR}$ is the free energy as calculated using eq 2 and $\lambda_s$ is the solvent reorganization energy.

If the excited DAC is formed upon excitation at the maximum of the CT band, the initial value of $X$ is 1, and it decreases to zero as solvent relaxation occurs (see Figure 6A). Barbara and co-workers have described the time dependence of $X$ by an exponential function decaying to zero with a time constant equal to the diffusional solvation time.[23]

As discussed above, recent investigations have emphasized the role of inertial motion in solvation,[47−49] and therefore, this ultrafast contribution has to be taken into account in the time dependence of $X$. Moreover, structural changes involving diffusion are also taking place. As these changes seem to be assisted by solvation, it is reasonable to include the corresponding reorganization energy in $\lambda_s$. To take these changes and inertial motion into account, the time dependence of $X$ is described as

$$X(t) = x_{is}\exp(-t/\tau_{is})^2 + x_{ds}\exp(-t/\tau_{ds}) + x_{sc}\exp(-t/\tau_{sc}) \quad (5)$$

where $x_{is}$, $x_{ds}$, and $x_{sc}$ are the relative amplitudes of the contribution to $\lambda_s$ of inertial solvation, diffusive solvation and structural changes, respectively, and their sum is equal to unity.

The magnitude of $\lambda_s$ for the D/PMDA DACs is not known. It can be, in principle, deduced from absorption band shape analysis. However, as stated above, only the low energy side of the CT band is available and therefore an analysis that takes vibronic transitions into account cannot be performed.

The most typical literature value of $\lambda_{hf}$ and $\lambda_s$ for DACs in polar solvents is of the order of 0.25 and 0.5 eV, respectively.[12] Assuming that $\lambda_{lf}$ is of the order of 0.1 eV, the total reorganization energy amounts to 0.85 eV.

Figure 7 shows the time evolution of the excited DAC population in ACN calculated with a $X$ dependent CR rate constant as expressed by eq 3. For the calculation, $x_{is}$, $x_{ds}$, and $x_{sc}$ were taken as 0.45, 0.45, and 0.1, respectively and time constants of 190 fs,[65] 500 fs and 11 ps were used for $\tau_{is}$, $\tau_{ds}$, and $\tau_{sc}$, respectively. The aim of this simulation was to reproduce the excited-state lifetime measured with DMB/PMDA in ACN. However, to obtain a 500 fs lifetime, a $V$ value of 1.5 eV had to be used! The magnitude of this value can be understood by considering that, with $\lambda$ = 0.85 eV and $\Delta G_{CR}$ = − 1.91 eV, the CR is deeply in the inverted regime and thus ultrafast CR is only possible with a very large electronic coupling matrix element.

Contrarily to the observation, the calculated time profiles are nonexponential, especially at early time. Consequently, the excited-state lifetime was calculated as

$$\tau_e = \frac{1}{N_e(0)}\int_0^\infty N_e(t)dt \quad (6)$$

where $N_e$ is the excited-state population. This nonexponential behavior is connected to the $X$ dependence of $k_{CR}$. At time zero, $X$ = 1, the activation energy for CR is very large and therefore CR is slow. As solvation occurs, the activation energy diminishes and $k_{CR}$ increases. Therefore, some solvation is needed before CR can really become operative. As a consequence, the population stays almost constant during the first few tens of fs. The length of this period depends strongly on the magnitude of $\partial\Delta G^{\ddagger}_{CR}/\partial X$. Figure 7 shows that if a larger solvent reorganization energy is assumed ($\lambda_s$ = 0.8 eV), i.e., if the process is less in the inverted region, a smaller $V$ is required. However, the

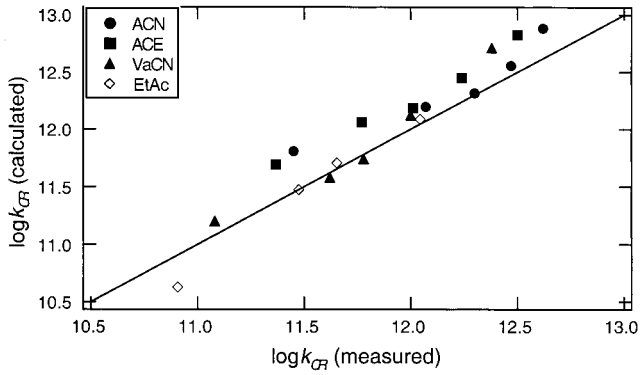


**Figure 8.** Comparison of the calculated and measured CR rate constants in all four solvents.

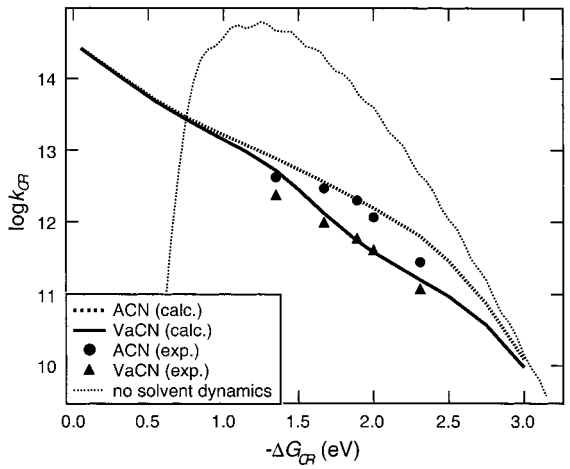


**Figure 9.** Free energy dependence of the CR rate constant calculated using the hybrid model in ACN, in VaCN and assuming an instantaneous solvent response.

excited population decay is further from exponential, because $\lambda_s$ and $\partial\Delta G^{\ddagger}_{CR}/\partial X$ are larger.

One way to obtain a more exponential decay, is to assume a larger intramolecular reorganization energy because this parameter does not depend on $X$. A larger $\lambda_{hf}$ also allows to reproduce a 500 fs lifetime with a more reasonable $V$ value. Figure 7 shows the population decay using $\lambda_s = 0.8$ eV and $\lambda_{hf} = 0.4$ eV. With these parameters, a decay time $\tau_e$ of 500 fs is obtained with $V = 0.2$ eV, which is much more realistic. Recently, $\lambda_{hf}$ and $\lambda_s$ values of 0.4 and 0.86 eV, respectively, have been found from the analysis of the free energy dependence of the CR dynamics of GIPs formed by ET quenching of cyanoanthracene derivatives by MoBs. It was found that the GIPs were closer to CIPs than to solvent separated ion pairs,[28] and therefore is it reasonable to assume similar $\lambda$ values for the DACs investigated here.

Figure 8 shows a plot of the calculated CR rate constant ($k_{CR}$ (calc) $= 1/\tau_e$) as a function of the $k_{CR}$ values measured in the four solvents. The calculation has been performed with $\lambda_{hf} = 0.4$ eV, $\lambda_{lf} = 0.1$ eV and with $\lambda_s = 0.5$ eV in EtAc and $\lambda_s = 0.8$ eV in the other solvents. The only difference between the solvents was the value of $\tau_{ds}$, which is listed in Table 1 and that of $\tau_{sc}$, which was taken as 11, 8, 35, and 50 ps in ACN, ACE, VaCN, and EtAc, respectively.

Both the observed free energy and the solvent dependence of $k_{CR}$ are qualitatively well reproduced. An even better agreement could certainly been obtained by slightly changing $V$, $\lambda_s$, $\lambda_{hf}$ and $\lambda_{lf}$. Moreover, it is also known that these parameters can somewhat vary from one DAC to another.[12,28]

Figure 9 shows the free energy dependence of $k_{CR}$ in ACN and VaCN calculated using the hybrid model over a large range of driving force. Three regimes can be distinguished:

(I) In the deep inverted region ($\Delta G_{CR} < -3$ eV), CR is slower than diffusional solvation. In this case, CR is not affected by dynamic solvent effects and can be described using the conventional nonadiabatic ET model.[66]

(II) In the $-3$ eV $< \Delta G_{CR} < -1.5$ eV region, CR can occur out of equilibrium. Inertial solvation alone is not sufficient to lower $X$ and $\Delta G^{\ddagger}_{CR}$ enough and some diffusional solvation has to occur before CR can take place. In this case, CR depends substantially on the diffusional solvation dynamics. Consequently, CR is slower in VaCN than in ACN.

(III) In the low exergonicity region ($\Delta G_{CR} > -1.5$ eV), inertial solvation alone can lower $\Delta G^{\ddagger}_{CR}$ sufficiently to reach the situation where CR is faster than diffusional solvation. If inertial dynamics is the same in both ACN and VaCN, as assumed here, $k_{CR}$ is no longer solvent dependent. In the limit where the driving force is very small, no solvation is even required to enter the ultrafast CR regime. As the equilibrium configuration of the reactant is never reached, the normal region, where $k_{CR}$ increases with increasing driving force, is not observed (see Figure 6B).

The absence of normal region depends strongly on the magnitude of $V$. If $V$ is smaller than about 0.1 eV, the excited state population cannot decay completely to the ground state before reaching the bottom of the excited-state potential surface. Consequently, the fraction of the excited population that is "trapped" in the equilibrium configuration has to overcome an activation barrier to recombine (see Figure 6B). In this case, the population dynamics is biphasic with an ultrafast component, corresponding to nonequilibrium CR, and a much slower component due to the thermally activated CR from the equilibrium configuration.

The CR rate constant will probably not reach the value of $10^{14}$ s$^{-1}$ shown in Figure 9. In this ultrafast regime, vibrational relaxation, which has been assumed here to be instantaneous, should certainly play a role in the CR dynamics. Therefore, the actual free energy dependence can be expected to start to saturate around $10^{13}$ s$^{-1}$. The departure from the linear free energy dependence of log$k_{CR}$ measured with the stronger donors in ACN and ACE might be a manifestation of this effect.

**Temperature Dependence of $k_{CR}$.** As shown in Table 5, the small activation energy related to CR depends apparently on the driving force. Such a relationship is also predicted by the hybrid model, assuming that the temperature dependence of $X$ is essentially due to $\tau_{ds}$ and $\tau_{sc}$, which are both diffusional processes. Figure 10 shows that, although the measured temperature dependence of $k_{CR}$ is somewhat larger than that predicted, the free energy dependence of the activation energy is qualitatively well reproduced. In the simulation, the inertial solvent motion has been assumed to be temperature independent. This might not be totally true[65] and could somehow contribute to the difference between the observed and the calculated activation energies.

The effect of temperature on $\tau_e$ depends on the relative time scale of CR and diffusional solvation and the above classification in three free energy regions can be used. In regime I, CR is independent of the solvent dynamics and exhibit almost no temperature dependence. In regime II, both diffusive solvation and CR are entangled and the effective activation energy for CR is a fraction of that related to the solvent viscosity. In regime III, CR is faster than diffusional solvation and is therefore almost independent of temperature. The small activation energy

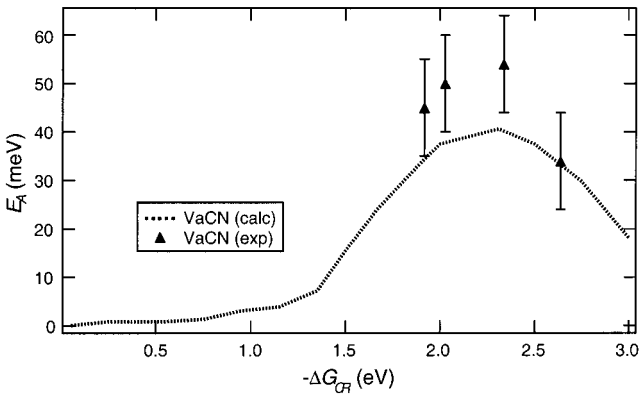


**Figure 10.** Calculated and measured activation energy for CR in VaCN.

observed with PXY/PMDA in VaCN could be explained by the fact that this system is close to regime I, contrarily to the MoB/PMDA DACs, which are rather in regime II.

**Differences between MeBs and MoBs.** The CR dynamics of MoB/PMDA is substantially faster than that of MeB/PMDA. This is not only due to the better electron donor properties of MoBs. Indeed, ANI and durene (DUR) have the same oxidation potential, and CR of ANI/PMDA is three times faster than that of DUR/PMDA.[13] The difference is even stronger when weaker electron acceptors are used: $k_{CR}$ ratio of ANI/A and DUR/A is 6 and 9 when A is tetracyanoanthracene and dicyanoanthracene, respectively.[27,28]

Interestingly, MoBs and MeBs also behave differently in forward ET quenching. In this case however, MoBs are less efficient quenchers than MeBs.[67,68]

This difference could possibly be due to different vibrational reorganization energies. The magnitude of this energy can be estimated from the difference between the vertical and the adiabatic ionization energy of the donor, $\Delta IP$.[69] For MoBs, $\Delta IP$ is of the order of 0.4 eV,[70] whereas for MeBs it is less than 0.1 eV. The effect of a larger vibrational reorganization energy is first, to attenuate the steepness of the inverted region and second, to shift the bell-shape curve to higher exergonicity. This results in an acceleration of the CR, because this process occurs in the inverted region and in a decrease of the forward ET rate constant, because this process takes place in the normal region. Of course, differences in other parameters, such as $V$, cannot be excluded.

## Concluding Remarks

The above discussion shows that the free energy, the solvent and the temperature dependence of the CR dynamics of excited MoBs/PMDA DACs are qualitatively well described with the hybrid model of Barbara and co-workers.[23] However, a major prediction of this model, i.e., the nonexponential decay of the excited state population was not really observed. The reason for this discrepancy is not clear and might be due to the fact that spectral changes occurring in the same time scale as solvent relaxation are somehow influencing the measured time profiles. For example, the initial rise observed experimentally can only be reproduced if an increase of the oscillator strength of the transition responsible for the 670 nm band of $PMDA^{\bullet-}$ upon solvation and/or structural changes of the excited DAC is assumed.

Moreover, the electronic coupling matrix element $V$ has been assumed to be constant in the above analysis. However, solvent induced structural changes might also affect $V$. For example, solvation of the excited DAC may result to a slight increase of the interionic distance and hence to a parallel decrease of $V$. Such an effect would make the decay of the excited-state population less nonexponential.

Temperature has also been assumed to be constant. This is certainly not entirely correct, and the effect of the vibrational temperature on the excited-state dynamics would be a worthwhile investigation.

A major difference between our description of $X(t)$ and previous studies is the contribution of inertial motion to solvation. In our simplified analysis, the amplitude of this contribution was assumed to be the same in all solvents, but this is certainly sufficient to gain some qualitative understanding of its role on the CR dynamics. If the decay of $X$ via inertial motion is not taken into account, the nonexponentiality of the population decay is even stronger and unrealistically large $V$ values have to be invoked to account for the ultrafast CR.

Finally, this model offers an explanation for the absence of normal region, which is qualitatively similar to that proposed by Tachiya and Murata,[17] except that in the latter case, inertial solvation was not taken into account.

It is clear that this low exergonicity region deserves further detailed investigation.

**Acknowledgment.** The authors would like to thank Prof. Anatoli Ivanov for helpful discussion and comments on the manuscript. This work was supported by the fonds National Suisse de la Recherche Scientifique though Project No. 2000-0632528.00.

## References and Notes

(1) *Photoinduced Electron Transfer*; Fox, M. A., Chanon, M., Eds.; Elsevier: Amsterdam, 1988.
(2) *Electron Transfer: From Isolated Molecules to Biomolecules*; Jortner, J., Bixon, M., Eds.; J. Wiley: New York, 1999; Vol. 106.
(3) *Electron Transfer in Chemistry*; Balzani, V., Ed.; J. Wiley: New York, 2001.
(4) Gould, I. R.; Young, R. H.; Moody, R. E.; Farid, S. *J. Phys. Chem.* **1991**, *95*, 2068.
(5) Itoh, M.; Mimura, T. *Chem. Phys. Lett.* **1974**, *24*, 551.
(6) Myers, A. B. *Chem. Phys.* **1994**, *180*, 215.
(7) Asahi, T.; Mataga, N. *J. Phys. Chem.* **1989**, *93*, 6575.
(8) Ojima, S.; Myasaka, H.; Mataga, N. *J. Phys. Chem.* **1990**, *94*, 7534.
(9) Asahi, T.; Mataga, N.; Takahashi, Y.; Miyashi, T. *Chem. Phys. Lett.* **1990**, *171*, 309.
(10) Asahi, T.; Mataga, N. *J. Phys. Chem.* **1991**, *95*, 1956.
(11) Hubig, S. M.; Bockman, T. M.; Kochi, J. K. *J. Am. Chem.* **1996**, *118*, 3842.
(12) Gould, I. R.; Noukakis, D.; Gomez-Jahn, L.; Goodman, J. L.; Farid, S. *J. Am. Chem. Soc.* **1993**, *115*, 4405.
(13) Asahi, T.; Ohkohchi, M.; Mataga, N. *J. Phys. Chem.* **1993**, *97*, 13 152.
(14) Miyasaka, H.; Kotani, S.; Itaya, A.; Schweitzer, G.; Schryver, F. C. D.; Mataga, N. *J. Phys. Chem. B* **1997**, *101*, 7978.
(15) Mataga, N.; Asahi, T.; Kanda, Y.; Okada, T.; Kakitani, T. *Chem. Phys.* **1988**, *127*, 249.
(16) Levin, P. P.; Pluzhnikov, P. F.; Kuzmin, V. A. *Chem. Phys. Lett.* **1988**, *147*, 283.
(17) Tachiya, M.; Murata, S. *J. Am. Chem. Soc.* **1994**, *116*, 2434.
(18) Frantzusov, P. A.; Tachiya, M. *J. Chem. Phys.* **2000**, *112*, 4216.
(19) Yoshihara, K.; Tominaga, K.; Nagasawa, Y. *Bull. Chem. Soc. Jpn.* **1995**, *68*, 696.
(20) Nagasawa, Y.; Yartsev, A. P.; Tominaga, K.; Bisht, P. B.; Johnson, A. E.; Yoshihara, K. *J. Phys. Chem.* **1995**, *99*, 653.
(21) Reid, P. J.; Barbara, P. F. *J. Phys. Chem.* **1995**, *99*, 3554.
(22) Johnson, A. E.; Levinger, N. E.; Jarzeba, W.; Schlief, R. E.; Kliner, D. A. V.; Barbara, P. F. *Chem. Phys.* **1993**, *176*, 555.
(23) Walker, G. C.; Akesson, E.; Johnson, A. E.; Levinger, N. E.; Barbara, P. F. *J. Phys. Chem.* **1992**, *96*, 3728.
(24) Tominaga, K.; Kliner, D. A.; Johnson, A. E.; Levinger, N. E.; Barbara, P. F. *J. Chem. Phys.* **1993**, *98*, 1228.
(25) Barbara, P. F.; Walker, G. C.; Smith, T. P. *Science* **1992**, *256*, 975.
(26) Riddick, J. A.; Bunger, W. B. *Organic Solvents*; J. Wiley: New York, 1970.

(27) Vauthey, E.; Högemann, C.; Allonas, X. *J. Phys. Chem. A* **1998**, *102*, 7362.
(28) Vauthey, E. *J. Phys. Chem. A* **2001**, *105*, 340.
(29) Gumy, J. C.; Nicolet, O.; Vauthey, E. *J. Phys. Chem. A* **1999**, *103*, 10 737.
(30) Gumy, J.-C. PhD Thesis, University of Fribourg, 2000.
(31) Poigny, S.; Guyot, M.; Samadi, M. *Tetrahedron* **1998**, *54*, 14 791.
(32) Perrin, D. D.; Armarego, W. L. F.; Perrin, D. R. *Purification of Laboratory Chemicals*; Pergamon Press: Oxford, 1980.
(33) Job, P. *Ann. Chim.* **1928**, *9*, 113.
(34) Wosburgh, W. C.; Cooper, G. R. *J. Am. Chem. Soc.* **1941**, *63*, 437.
(35) Weinberg, N. L.; Weinberg, H. R. *Chem. Rev.* **1968**, *68*, 449.
(36) Murov, S. L.; Carmichael, I.; Hug, G. L. *Handbook of Photochemistry*; Marcel Dekker: New York, 1993.
(37) Högemann, C.; Pauchard, M.; Vauthey, E. *Rev. Sci. Instrum.* **1996**, *67*, 3449.
(38) Fourkas, J. T.; Trebino, R.; Fayer, M. D. *J. Chem. Phys.* **1992**, *97*, 69.
(39) Shida, T.; Iwata, S.; Imamura, M. *J. Phys. Chem.* **1974**, *78*, 741.
(40) Andruniow, T.; Pawlikowski, M.; Zgierski, M. Z. *J. Phys. Chem. A* **2000**, *104*, 845.
(41) Vauthey, E. In *Ultrafast Phenomena XII*; Elsaesser, T., Mukamel, S., Murnane, M. M., Scherer, N. F., Eds.; Springer: Berlin, 2000; p 485.
(42) Huddleston, R. K.; Miller, J. R. *J. Phys. Chem.* **1982**, *86*, 2410.
(43) Hush, N. S. *Prog. Inorg. Chem.* **1967**, *8*, 391.
(44) Laermer, F.; Elsaesser, T.; Kaiser, W. *Chem. Phys. Lett.* **1989**, *156*, 381.
(45) Kovalenko, S. A.; Schanz, R.; Henning, H.; Ernsting, N. P. *J. Chem. Phys.* **2001**, *115*, 3256.
(46) Miyasaka, H.; Hagihara, M.; Okada, T.; Mataga, N. *Chem. Phys. Lett.* **1992**, *188*, 259.
(47) Rosenthal, S. J.; Xie, X.; Du, M.; Fleming, G. R. *J. Chem. Phys.* **1991**, *95*, 4715.
(48) Maroncelli, M.; Kumar, V. P.; Papazyan, A. *J. Phys. Chem.* **1993**, *97*, 13.
(49) Jimenez, R.; Fleming, G. R.; Kumar, P. V.; Maroncelli, M. *Nature* **1994**, *369*, 471.
(50) Horng, M. L.; Gardecki, J. A.; Papazyan, A.; Maroncelli, M. *J. Phys. Chem.* **1995**, *99*, 17 311.
(51) Weller, A. *Pure Appl. Chem.* **1982**, *54*, 1885.
(52) Jarzeba, W.; Murata, S.; Tachiya, M. *Chem. Phys. Lett.* **1999**, *301*, 347.
(53) Vauthey, E., unpublished results.
(54) Sivakumar, N.; Hoburg, E. A.; Waldeck, D. H. *J. Chem. Phys.* **1989**, *90*, 2305.
(55) Mataga, N.; Miyasaka, H. *Adv. Chem. Phys.* **1999**, *107*, 431.
(56) Vauthey, E. *J. Phys. Chem.* **2000**, *104*, 1804.
(57) Vauthey, E.; Parker, A. W.; Nohova, B.; Phillips, D. *J. Phys. Chem.* **1994**, *116*, 9182.
(58) Gould, I. R.; Farid, S. *J. Am. Chem. Soc.* **1988**, *110*, 7883.
(59) Muller, P.-A.; Högemann, C.; Allonas, X.; Jacques, P.; Vauthey, E. *Chem. Phys. Lett.* **2000**, *236*, 321.
(60) Kulinowski, K.; Gould, I. R.; Ferris, N. S.; Myers, A. B. *J. Phys. Chem.* **1995**, *99*, 17 715.
(61) Arnold, B. R.; Farid, S.; Goodman, J. L.; Gould, I. R. *J. Am. Chem. Soc.* **1996**, *118*, 5482.
(62) Weller, A. *Z. Phys. Chem. N. F.* **1982**, *133*, 93.
(63) Sumi, H.; Marcus, R. A. *J. Chem. Phys.* **1986**, *84*, 4894.
(64) Jortner, J.; Bixon, M. *J. Chem. Phys.* **1988**, *88*, 167.
(65) Passino, S. A.; Nagasawa, Y.; Fleming, G. R. *J. Phys. Chem.* **1997**, *101*, 725.
(66) Marcus, R. A.; Sutin, N. *Biochim. Biophys. Acta* **1985**, *811*, 265.
(67) Jacques, P.; Allonas, X.; von Roumur, M.; Suppan, P.; Haselbach, E. *J. Photochem. Photobiol. A* **1999**, *111*, 41.
(68) Dossot, M., Burget D., Allonas X., Jacques P. *N. J. Chem.* **2001,** *25*, 194.
(69) Nelsen, S. In *Advances in Electron-Transfer Chemistry 3*; Mariano, P. S., Ed.; JAI Press Inc.: Greenwich, 1993; Vol. 3; p 167.
(70) Jacques, P.; Allonas, X.; Burget, D.; Haselbach, E.; Muller, P.-A.; Sergenton, A.-C.; Galliker, H. *Phys. Chem. Chem. Phys.* **1999**, *1*, 1867.